Mn^{2+} centres induced by hydrolysis processes in BaF_2:Mn: EPR study

1989 J. Phys.: Condens. Matter 1 8217

(http://iopscience.iop.org/0953-8984/1/43/021)

J. Phys.: Condens. Matter 1 (1989) 8217–8226. Printed in the UK

Mn^{2+} centres induced by hydrolysis processes in BaF_2: Mn: an EPR study

R Alcalá, J I Peña and P J Alonso

Instituto de Ciencia de Materiales de Aragón, Universidad de Zaragoza–Consejo Superior de Investigaciones Científicas, Facultad de Ciencias, Pz S Francisco s/n, 50009 Zaragoza, Spain

Received 27 January 1989, in final form 29 March 1989

Abstract. Changes in the EPR spectra of manganese-doped BaF_2 single crystals induced by thermal treatments in different atmospheres have been studied. No modifications have been induced by thermal treatments at temperatures below 500 °C. Annealings above 700 °C only induce a total destruction of the cubic Mn^{2+} signal (Mn^{2+}–I). If the annealings are performed at temperatures between 500 and 700 °C the modifications of the EPR spectra depend on the presence of water vapour in the surrounding atmosphere. When the annealing is performed in dry oxygen or nitrogen only the trigonal Mn^{2+}–II centre, which has already been reported by Orera *et al*, is formed. If the annealings are performed in a wet atmosphere, two new manganese-related centres are formed. One of them has a trigonal symmetry and shows a resolved superhyperfine interaction with one fluorine. The other one has an orthorhombic symmetry and does not show any superhyperfine structure. Values of the spin-Hamiltonian parameters for both centres are given. A study of the production conditions and interconversion of the different centres is presented. Some tentative models for each are discussed.

1. Introduction

Alkaline-earth fluorides are easily hydrolysed by heating the crystals in a moist atmosphere at high temperature. Then hydroxyl and oxygen impurities are incorporated into the samples (Bontinck 1958, Wickersheim and Hanking 1959, Bollmann 1980, Deyhimi and Bill 1982, Catlow 1977, Kumar 1982, Peña *et al* 1988). The equilibrium of the bulk reaction of OH^- with fluorine ions giving oxygen–vacancy pairs and HF molecules explains the presence of both types of impurities (Catlow 1977, Kumar 1982, Peña *et al* 1988). This equilibrium can be modified by adding foreign impurities as found in the case of rare-earth (RE)-doped alkaline-earth fluorides (Sierro 1961, Reddy *et al* 1971, Catlow 1977, Nakata *et al* 1979). Rare-earth ions enter these fluorides as RE^{3+} in a cation site and interstitial fluorine ions (F_i^-) act as charge compensators. The reaction of bulk OH^- ions with this F_i^- giving out HF molecules and substitutional O^{2-} ions explains the low concentration of hydroxyl impurities in RE-doped crystals as compared with the pure ones after thermal annealing in a wet atmosphere (Catlow 1977).

On the other hand, manganese impurities enter these crystals as Mn^{2+} in a cation site and no charge compensation is needed. This Mn^{2+} centre has been studied by EPR and a resolved superhyperfine structure due to the interaction with eight fluorine nuclei

0953-8984/89/438217 + 10 $02.50

at the corners of a cube has been observed (Richardson *et al* 1972). This centre appears in *as-grown* samples and it will be labelled as Mn^{2+}–I in the following.

Other Mn^{2+} centres have been studied by EPR in CaF_2 and SrF_2 crystals, some of them with a point symmetry lower than cubic (Lay and Nolle 1967, Reddy 1971, Van Gorkom 1970, Nakata *et al* 1976, Alcalá *et al* 1983, Alonso and Alcalá 1985). In all cases the number of fluorines in the first coordination shell, which is responsible for the resolved superhyperfine structure, is lower than in the Mn^{2+}–I centre. These facts have been associated with the trapping of fluorine vacancies, hydroxyl ions and oxygen ions in the neighbourhood of Mn^{2+}. The relation between hydrolysis processes in SrF_2:Mn and the formation of Mn^{2+} centres different from Mn^{2+}–I has been reported recently (Alonso *et al* 1988). In the present paper we study the EPR spectra of various Mn^{2+} centres created in BaF_2:Mn by thermal annealing in different atmospheres. One of these centres, produced by annealing in a dry atmosphere, coincides with that reported by Orera *et al* (1984). The other two, labelled Mn^{2+}–IV and Mn^{2+}–V are only formed after annealing in a wet atmosphere at temperatures between 500 and 700 °C, and modifications of the optical absorption spectrum in the 3000–4000 cm^{-1} region are observed. The EPR spectra of both defects have been analysed as well as their interconversion under thermal treatments. Tentative models for the new Mn^{2+} centres are also discussed.

2. Experimental procedure

BaF_2 single crystals have been kindly provided by Dr H W den Hartog (Solid State Physics Laboratory, Groningen, The Netherlands). Three different batches were used with a manganese content in the raw material of 0.17, 0.29 and 0.63 mol%. Our results were independent of the Mn^{2+} content.

Optical absorption measurements were taken in a 783 Perkin-Elmer IR spectrophotometer. EPR spectra were recorded at liquid nitrogen temperature (LNT) using an immersion quartz Dewar in an E-112 Varian spectrometer working in the X band. Magnetic fields were measured with a Bruker ER 035M NMR gaussmeter and the microwave frequency was determined from the diphenylpicrylhydrazyl (DPPH) resonance line ($g = 2.0037 \pm 0.0002$).

Thermal annealings in flowing oxygen or nitrogen gave the same results. The samples were placed in an open quartz tube heated by a conventional furnace. Dry oxygen or nitrogen atmospheres were obtained by bubbling the gases through H_2SO_4. In order to obtain a wet atmosphere the gases were passed through distilled water (D_2O was used in some cases). A static atmosphere cannot be used for annealing in a dry atmosphere because of the release of adsorbed water from the quartz walls (Deyhimi and Bill 1982).

3. Experimental results

The EPR spectra of untreated BaF_2:Mn samples show only the signal corresponding to Mn^{2+} ions in a cation substitutional position (Richardson *et al* 1972). These centres will hereafter be called Mn^{2+}–I centres. The optical absorption spectrum of these samples does not show any absorption between 50 000 cm^{-1} and 700 cm^{-1}. The electronic transitions of Mn^{2+}–I in this region are between states of the 3d configuration and then are both spin and parity forbidden. Consequently they have a very low oscillator strength.

Depending on the temperature and the water content of the surrounding atmosphere, these spectroscopic properties are modified by annealing the BaF_2:Mn samples. For comparison, pure BaF_2 samples have also been annealed in the same conditions as the doped ones. Some of the effects of these annealings can be erased by polishing the samples (Peña *et al* 1988). Thus the following experiments involve samples that have been polished after thermal treatment and only bulk defects induced by the hydrolysis processes have been taken into account.

Annealings at temperatures below 500 °C induce no change in the optical absorption nor in the EPR spectrum of either pure or manganese-doped BaF_2 samples regardless of the surrounding atmosphere. Thermal annealings at higher temperatures produce some modifications of these spectroscopic properties.

For pure samples no new EPR signals have been found after thermal annealing whatever the temperature or surrounding atmosphere. If the annealings are performed in a wet atmosphere above 500 °C the formation of an absorption band at 3630 cm^{-1} (halfwidth 10 cm^{-1}) is observed, arising from the stretching mode of free hydroxyl ions (OH^-) in the samples (Peña *et al* 1988).

Annealing of BaF_2:Mn crystals at temperatures higher than 500 °C produces a decrease of the Mn^{2+}–I signal in all cases, and at temperatures higher than 700–750 °C the Mn^{2+}–I signal completely disappears. So we restrict ourselves to the spectroscopic modifications in the BaF_2:Mn samples following annealings at temperatures between 500 and 700°C.

Annealings in a dry atmosphere (dry oxygen or dry nitrogen) produce no changes in the optical absorption spectrum and no evidence of OH^- ions. Nevertheless, a decrease of the Mn^{2+}–I EPR signal together with the formation of a new paramagnetic manganese-related centre is observed after thermal annealing at temperatures between 600 and 700 °C followed by a quick cooling to room temperature (RT). This EPR signal coincides with the one described by Orera *et al* (1984) which is assigned to a Mn^{2+} ion in a trigonal environment (this centre is labelled as Mn^{2+}–II). These authors form the Mn^{2+}–II signal by thermal treatment at about 625 °C in a water-free argon atmosphere.

BaF_2:Mn samples thus treated and showing the Mn^{2+}–I and Mn^{2+}–II EPR signals have been annealed at progressively higher temperatures above RT for a short time. No modifications of the spectra are induced below 300 °C but at higher temperatures a strong decrease of the Mn^{2+}–II EPR signal together with a recovery of the Mn^{2+}–I one is observed.

After annealings in a wet atmosphere the modifications of the spectroscopic properties are more complex and two new paramagnetic centres are formed. These two centres will be labelled as Mn^{2+}–IV and Mn^{2+}–V. (For another centre labelled Mn^{2+}–III see Orera *et al* (1984).) At the same time different absorption bands in the 3000–4000 cm^{-1} IR region are observed. We will first describe the changes observed in the EPR spectra.

After annealing in wet oxygen or nitrogen at temperatures in the range 500–600 °C the EPR signal of a new manganese centre (Mn^{2+}–IV) is observed. The intensity of the Mn^{2+}–IV signal decreases when the quenching rate of the sample from 600 °C to RT increases. Occasionally the Mn^{2+}–II signal also appears, especially when the sample is quickly quenched down to RT. The Mn^{2+}–IV signal mainly consists of several groups of six doublets with a mean splitting between each of these doublets of about 8.5 mT due to the hyperfine interaction with the manganese nucleus (^{55}Mn, $I = \frac{5}{2}$, natural abundance 100%). Each of the six doublets consists of two lines of the same intensity with a peak-to-peak distance of about 0.9 mT and with a splitting between them that varies from 2.6 mT to 1.4 mT depending on the magnetic field orientation. This further splitting

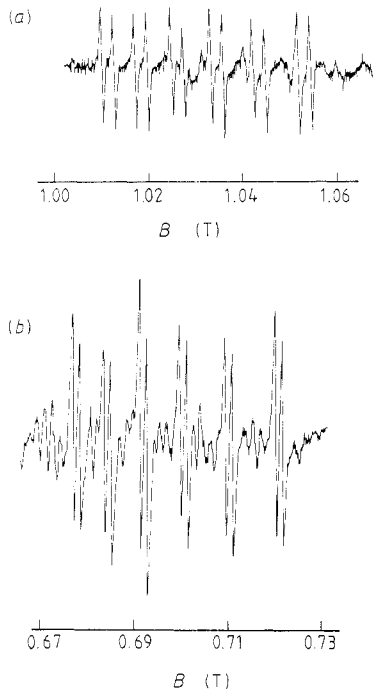

Figure 1. High-field sextets of the Mn^{2+}–IV EPR signal taken with the magnetic field along the ⟨111⟩ (*a*) and ⟨110⟩ (*b*) crystal axis.

indicates a superhyperfine (SHF) interaction with an $I = \frac{1}{2}$ nucleus. To distinguish between F^- and OH^- some samples were prepared by annealing in D_2O. The SHF pattern does not change, indicating that it is due to interaction with one ^{19}F nucleus. We show in figure 1 the higher-field sextets of the Mn^{2+}–IV signal measured at liquid nitrogen temperature (LNT) with the magnetic field along the ⟨111⟩ (*a*) and ⟨110⟩ (*b*) directions.

The dependence of the Mn^{2+}–IV EPR signal on the magnetic field orientation has also been studied. The mean positions of the *sextets* as a function of the magnetic field orientation when it rotates in a {110} plane are shown in figure 2. Only few points can be given with enough accuracy due to overlapping problems and also because the intensities of the lines are strongly dependent on the magnetic field orientation, which is typical of systems with high crystal field terms combined with noticeable values of the hyperfine interaction (Bir 1964). In spite of this it can be seen that the symmetry of the Mn^{2+}–IV centre is trigonal with the threefold axis parallel (figure 1(*a*)) and perpendicular (figure 1(*b*)) to the magnetic field.

BaF_2:Mn samples quenched to RT after thermal annealing in a wet atmosphere at 600 °C have been annealed at progressively higher temperatures above RT. It is observed that annealing at about 100 °C induces an increase of the Mn^{2+}–IV signal together with a decrease of the Mn^{2+}–I signal. The intensities of the Mn^{2+}–I and Mn^{2+}–IV signals are restored by a further quenching to RT after annealing at temperatures above 300 °C for a short time (typically ten minutes).

Another divalent manganese centre (labelled as Mn^{2+}–V) is formed by annealing BaF_2:Mn samples in a wet atmosphere at about 700 °C followed by a slow cooling down to RT. The EPR signal corresponding to this defect consists of several *sextets* formed by six lines of the same intensity with a peak-to-peak distance of 0.8 mT. The mean distance between adjacent lines is about 8.5 mT. The evolution of this signal with the magnetic

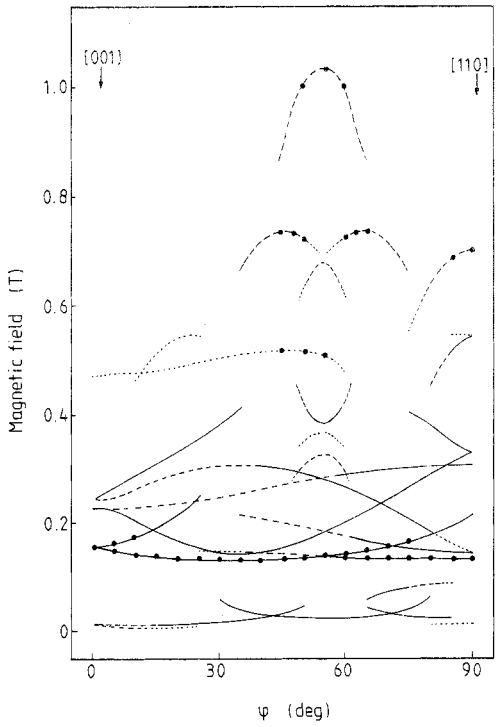

Figure 2. Full circles represent the mean position of the observed Mn^{2+}–IV sextets as a function of the magnetic field orientation in the (110) plane. Lines give the predicted evolution calculated using the spin-Hamiltonian given by equation (1) with the values of the parameters given in table 2. The angle φ is measured from the [001] direction.

field orientation has also been studied. It has been found that the intensities of the *sextets* are strongly dependent on the magnetic field orientation and no superhyperfine structure has been resolved for any orientation of the magnetic field. In figure 3(*a*) we represent the evolution of a mean position of these sextets when the magnetic field is rotated in the (001) plane. The corresponding evolution of the signal upon rotation of the magnetic field in the (110) plane is given in figure 3(*b*).

It is interesting to note that if, after a 700 °C annealing, the sample is quickly quenched to RT the EPR spectrum only shows the Mn^{2+}–IV signal instead of the Mn^{2+}–V one. A further annealing of these samples at about 100 °C induces the destruction of the Mn^{2+}–IV defects and the growth of the Mn^{2+}–V signal. This situation is reversed if the samples are annealed at temperatures above 300 °C and then quenched to RT.

Modifications of the optical absorption spectrum of BaF_2:Mn crystals are also produced by annealing at temperatures in the range 500–700 °C in a wet atmosphere. The formation of a free OH^- stretching-mode band (3630 cm^{-1}), which appears in the pure crystals, has not been detected in the Mn^{2+}-doped samples.

Instead, when thermal annealings are performed at temperatures in the range 500–600 °C a weak, broad band that extends approximately from 3000 cm^{-1} to 3800 cm^{-1} grows. The intensity of this band changes with thermal treatments in the same way as the intensity of the Mn^{2+}–IV EPR signal. In samples annealed at temperatures between 600 and 700 °C a broad IR absorption band is also found. It seems that there is a correlation between the IR absorption band and the presence of Mn^{2+}–IV and Mn^{2+}–V centres in the crystals. However, since broad IR bands also appear in pure samples and its intensity in our crystals is small it is difficult to make a definitive assertion about this correlation.

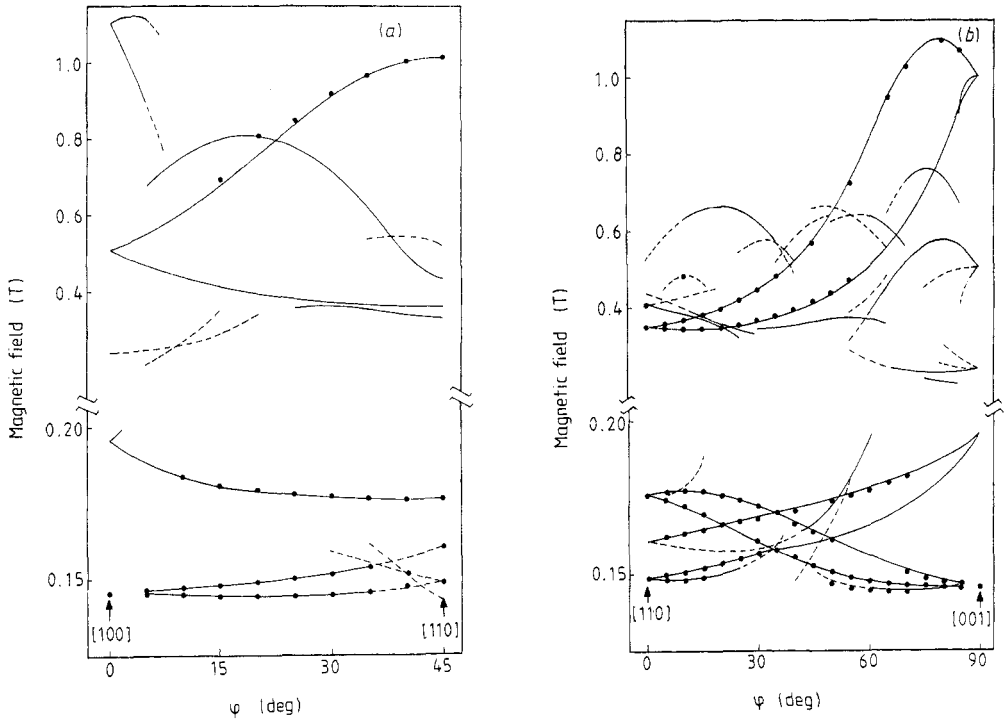

Figure 3. Full circles represent the mean position of the observed Mn^{2+} sextets as a function of the magnetic field orientation in the (001) (*a*) and in the (110) plane (*b*). Lines give the predicted evolution calculated using the spin-Hamiltonian given by equation (2) with the values of the parameters given in table 2. The angle φ is measured from the [100] direction (*a*) and from the [110] direction (*b*).

Table 1. Production conditions for the different Mn^{2+} centres.

Centre	Thermal treatment	Atmosphere
Mn^{2+}–I	Present in *as grown* crystals	
Mn^{2+}–II[a]	Quenching from 600 °C	Dry
Mn^{2+}–III[b]	Quenching from 900 °C	Dry
Mn^{2+}–IV[a]	Slow cooling from 600 °C	Wet
Mn^{2+}–V[a]	Slow cooling from 700 °C	Wet

[a] Present work.
[b] Orera *et al* (1984).

The production conditions for each Mn^{2+} centre found in BaF_2 are summarised in table 1.

4. Discussion

Thermal annealings of manganese-doped BaF_2 above 500 °C produce a decrease of the manganese content of the crystals regardless of the surrounding atmosphere. This can

Table 2. Spin-Hamiltonian parameters for the different Mn^{2+} centres found in BaF_2. Crystal field coefficients and the hyperfine constants are given in MHz. The signs of b_n^m have been estimated assuming that the isotropic hyperfine constant is negative.

Centre	Symmetry	g	b_2^0	b_2^2	$A_\parallel$	$A_\perp$
I[a]	cubic	2.0013	—	—	−273.7	
II[b]	trigonal	2.00	−2725	—	−265	
III[b]	orthorhombic	2.00	2430	1710	−265	
IV[c]	trigonal	2.00	4966	—	−241	−236
V[c]	orthorhombic	2.00	5408	−4152	−234	−226

[a] Richardson *et al* (1972).
[b] Orera *et al* (1984).
[c] This work.

be understood as due to a diffusion of these ions out of the crystal, as observed in SrF_2: Mn (Alonso *et al* 1988) and in CaF_2: Mn (Lay and Nolle 1967) after annealing at high temperatures.

Thermal treatments at 500–700 °C induce the formation of new paramagnetic Mn^{2+} centres. After annealing in a dry atmosphere only the Mn^{2+}–II centres are formed; their EPR spectrum (Orera *et al* 1984) corresponds to a trigonal defect showing a superhyperfine interaction with four fluorines, three equivalent and the other one on the threefold axis. The values of the spin-Hamiltonian parameters are given in table 2 with those of another Mn^{2+}-related centre (Mn^{2+}–III). This is an orthorhombic defect showing interactions with four fluorines, which is obtained after a short annealing at 900 °C in a static argon atmosphere. This centre is not observed in our crystals, probably because of the different annealing conditions.

When annealing in a wet atmosphere, Mn^{2+}–IV and/or Mn^{2+}–V centres are obtained, depending on temperature and cooling rate. Their EPR spectra (see previous section) have not been reported previously, and we now analyse their EPR signals.

From figure 2 the Mn^{2+}–IV centre has trigonal symmetry with its threefold axis along one of the ⟨111⟩ crystal directions, with a resolved superhyperfine interaction with a fluorine on the C_3 axis. The usual spin-Hamiltonian describes its EPR spectra:

$$\mathcal{H} = g\mu_B \boldsymbol{S}\cdot\boldsymbol{B} + \tfrac{1}{3}b_2^0 O_2^0 + A_\perp(S_xI_x + S_yI_y) + A_\parallel S_zI_z + A_\perp^F(S_xI_x^F + S_yI_y^F) + A_\parallel^F S_zI_z^F. \quad (1)$$

Here $S = \frac{5}{2}$, μ_B is the Bohr magneton and O_m^n and b_m^n are the Steven's operators and crystal field parameters respectively. $A_\parallel$ and $A_\perp$ are the hyperfine constants of the interaction with the ^{55}Mn nucleus ($I = \frac{5}{2}$) and $A_\parallel^F$ and $A_\perp^F$ are the superhyperfine parameters for interaction with the ^{19}F nucleus ($I^F = \frac{1}{2}$). The z axis is along the threefold axis; the electronic Zeeman term is isotropic.

By fitting the line positions calculated using equation (1) to the experimental ones we obtain the values for the spin-Hamiltonian parameters of the Mn^{2+}–IV centre given in table 2. For the superhyperfine interaction $A_\parallel^F = 75$ MHz and $A_\perp^F = 42$ MHz. Good agreement with the experimental results in both positions and relative intensities has been obtained. A model for this defect showing the principal axis of the crystal field as well as the location of the fluorine responsible for the superhyperfine structure is shown in figure 4(*a*).

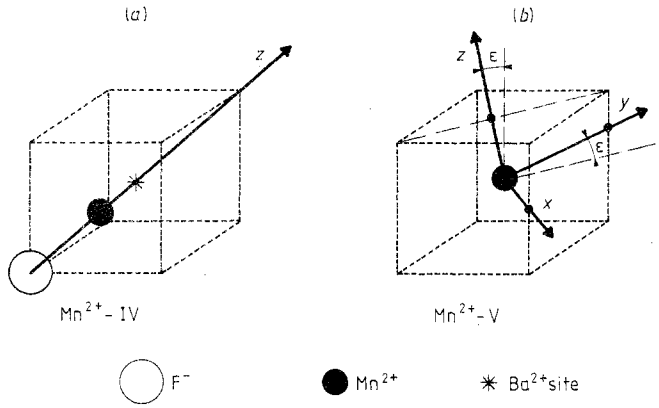

Figure 4. Sketches for the models of the Mn^{2+}–IV (*a*) and Mn^{2+}–V (*b*) centres showing the fluorine responsible for the observed superhyperfine structure and the orientation of the principal axis of the crystal field contribution to the spin-Hamiltonian.

The isotropic superhyperfine constant with the fluorine nucleus ($a_S^F = 53$ MHz) is noticeably higher than that of the fluorines of the first shell in the cubic Mn^{2+}–I centre ($a_S^F = 22.2$ MHz). This indicates that the Mn^{2+} ion is closer to the F^- in the Mn^{2+}–IV centre than in Mn^{2+}–I. In this last case (Mn^{2+}–I) Barriuso and Moreno (1984a), using a simple model (1984b), have estimated the $Mn^{2+}-F^-$ distance to be about 2.32 Å, corresponding to an inwards relaxation of the fluorine ions of about 14% in agreement with the smaller ionic radius of Mn^{2+} (0.80 Å) as compared with that of Ba^{2+} (1.34 Å). A similar calculation for Mn^{2+}–IV gives a value of about 2.09 Å for the Mn^{2+}–F^- distance, very close to that found in $KMnF_3$ (Wyckoff 1964) ($d_0 = 2.095$ Å) and also close to the sum of the ionic radii ($r_{F^-} + r_{Mn^{2+}} = 2.13$ Å).

For the Mn^{2+}–V centre the EPR spectrum shows that its symmetry is orthorhombic, with the spin-Hamiltonian

$$\mathcal{H} = g\mu_B \boldsymbol{S}\cdot\boldsymbol{B} + \tfrac{1}{3}(b_2^0 O_2^0 + b_2^2 O_2^2) + A_x S_x I_x + A_y S_y I_y + A_z S_z I_z \qquad (2)$$

where the various symbols are the same as in equation (1). No superhyperfine structure is resolved and the principal axes of the crystal field, depicted in figure 4(*b*), are the same for the hyperfine interaction described by an axial tensor ($A_x = A_y = A_\parallel$ and $A_z = A_\perp$).

The spin-Hamiltonian parameters of the Mn^{2+}–V centre are given in table 2 and the angle $\varepsilon = 11 \pm 1°$ is shown in figure 4(*b*).

The Mn^{2+}–IV and Mn^{2+}–V defects are only formed when the annealings are performed in an atmosphere containing water, so that hydroxyl and oxygen impurities are incorporated into the bulk through hydrolysis processes (Bontinck 1958, Wickersheim and Hanking 1959, Bollman 1980, Deyhimi and Bill 1982, Catlow 1977, Kumar 1982, Peña *et al* 1988). Centres involving both types of impurities, OH^- and O^{2-}, in their first coordination shell have been reported for RE-doped samples after hydrolysis (Sierro 1961, Reddy *et al* 1971, Nakata *et al* 1979).

In the case of Mn^{2+}-doped CaF_2 and SrF_2 crystals different Mn^{2+} centres with oxygen and perhaps OH^- ions close to the cationic impurity have also been reported (Lay and Nolle 1967, Reddy 1971, Van Gorkon 1970, Nakata *et al* 1976, Alonso *et al* 1988). From these considerations it seems to be clear that both OH^- and O^{2-} with or without a related fluorine vacancy can be involved in the structure of Mn^{2+}–IV and Mn^{2+}–V centres. On

the other hand, we have seen that there is some correlation between the IR absorption in the region 3000–3800 cm^{-1} and the Mn^{2+}–IV and Mn^{2+}–V EPR signals. It has been proposed by several authors that broad absorption bands in that region are due to perturbed OH^- ions. Because of this we tentatively propose that these two centres contain some OH^- ions associated with Mn^{2+}. These two defects seem to be closely related, as interconversion between Mn^{2+}–IV and Mn^{2+}–V is induced in a sample annealed at 700° C by thermal treatments at temperatures below 400 °C.

In spite of these considerations it is difficult to give a detailed model for Mn^{2+}–IV and Mn^{2+}–V defects with our present data. We tentatively propose that in Mn^{2+}–IV some of the eight fluorines that surround the Mn^{2+} site have been substituted by OH^- ions. Since we observe a superhyperfine interaction with one F^- we propose that only this fluorine remains in the Mn^{2+} first coordination shell, the other being substituted by OH^- ions. Other models involving a fluorine vacancy instead of the OH^- ion on the trigonal axis and even three oxygen–fluorine vacancy pairs instead of the other six hydroxyl ions are also compatible with the EPR observations.

For the Mn^{2+}–V centre our model is the same as for Mn^{2+}–IV but with one O^{2-} substituting for one of the OH^- ions placed out of the C_3 axis. This model accounts for the orthorhombic symmetry as well as for the close relationship between Mn^{2+}–IV and Mn^{2+}–V centres. On the other hand, the extra negative charge associated with the O^{2-} ions will induce a displacement of the Mn^{2+} away from the F^- ion, reducing the superhyperfine interaction to values lower than our experimental resolution (about 20 MHz). As for Mn^{2+}–IV, other models with no F^- in the first Mn^{2+} coordination shell together with an interstitial (either fluorine or hydroxyl) to give the right symmetry cannot be discarded.

Acknowledgments

We wish to thank Dr H W den Hartog (Solid State Physics Laboratory, Groningen, The Netherlands) for giving us the samples. One of us (JIP) wishes to thank DGA (local government of Aragón) for granting his stay at the Instituto de Ciencias de Materiales de Aragón. This research was sponsored by the Dirección General de Investigación Científica y Técnica under contract number PB0361 and by DGA under contract number P-IT-3188.

References

Alcalá R, Alonso P J and Cases R 1983 *J. Phys. C: Solid State Phys.* **16** 4693
Alonso P J and Alcalá R 1985 *Phys. Stat. Solidi* b **128** K153
Alonso P J, Peña J I and Alcalá R 1988 *J. Phys. C: Solid State Phys.* **21** 6029
Barriuso M T and Moreno M 1984a *Chem. Phys. Lett.* **112** 165
—— 1984b *Phys. Rev.* B **29** 3623
Bir G L 1964 *Sov. Phys.–Solid State* **5** 1628
Bollmann W 1980 *Phys. Stat. Solidi* a **57** 601
Bontinck W 1958 *Physica* **24** 650
Catlow C R A 1977 *J. Phys. Chem. Solids* **38** 1131
Deyhimi F and Bill H 1982 *J. Solid State Chem.* **43** 181
Kumar B 1982 *J. Am. Ceramic Soc.* **65** C-176
Lay F M T and Nolle A W 1967 *Phys. Rev.* **163** 266
Nakata R, Kawano K, Sumita M and Higuchi E 1976 *J. Phys. Soc. Japan* **41** 470

Nakata R, Kawano K, Sumita M and Higuchi E 1979 *J. Phys. Chem. Solids* **40** 955
Orera V M, Alcalá R and Alonso P J 1984 *Solid State Commun.* **50** 665
Peña J I, Alonso P J and Alcalá R 1988 *J. Phys. Chem. Solids* **49** 273
Reddy T Rs 1971 *Phys. Lett.* **36A** 11
Reddy T Rs, Davies E R, Baker J M, Chambers D N, Newman R C and Ozbay B 1971 *Phys. Lett.* **36A** 231
Richardson R J, Lee S and Menne T J 1972 *Phys. Rev.* B **6** 1065
Sierro J 1961 *J. Chem. Phys.* **34** 2183
Van Gorkom G G P 1970 *J. Phys. Chem. Solids* **31** 905
Wickersheim K A and Hanking B M 1959 *Physica* **25** 569
Wyckoff R W G 1964 *Crystal Structure* vol. 2 2nd edn (New York: Interscience) p 392